Structural Chemistry (2024) 35:65–73
https://doi.org/10.1007/s11224-023-02248-3

RESEARCH

A theoretical study of the reactivity of 5-fluorouracil toward superoxide radical anion and hydroperoxyl radical

Tatsushi Nakayama[1]

Received: 19 September 2023 / Accepted: 18 October 2023 / Published online: 23 October 2023

Abstract

The reactivity of 5-fluoro-1*H*,3*H*-pyrimidine-2,4-dione (5-fluorouracil), which is widely used to treat cancer, toward superoxide radical anion ($O_2^{\bullet-}$) and hydroperoxyl radical ($HO_2^{\bullet}$) was investigated using density functional theory (DFT) calculations. 5-Fluorouracil is a pyrimidine analog with cytotoxic effects on cancer cells and potential ecotoxicology as a recalcitrant compound to the natural environment; therefore, clarifying its chemical degradation mechanism is difficult by way of in vivo and in vitro experiments but important for further usage. The DFT results clarified that the oxidation of 5-fluorouracil by $O_2^{\bullet-}$ or $HO_2^{\bullet}$ in water is feasible through a proton-coupled electron transfer (PCET) mechanism. In addition, a concerted PCET pathway between 5-fluorouracil and $HO_2^{\bullet}$ preformed via the protonation of $O_2^{\bullet-}$ is proposed. In this pathway, the amine group at the first position of 5-fluorouracil acts as a reaction site for the concerted PCET after forming a prereactive complex via a hydrogen bond. Considering that the actual oxidant along the PCET pathways is $HO_2^{\bullet}$ with a short lifetime, the biodegradability of 5-fluorouracil by $O_2^{\bullet-}$ ($HO_2^{\bullet}$) is governed by the complex formation step and the concerted PCET.

Keywords 5-Fluorouracil · Pyrimidine base · Superoxide radical anion · Hydroperoxyl radical · Density functional theory · Proton-coupled electron transfer

Introduction

5-Fluoro-1*H*,3*H*-pyrimidine-2,4-dione (5-fluorouracil, 5-FU) is a cytotoxic chemotherapy medication used to treat cancer and belongs to the antimetabolite and pyrimidine analog families of medications [1–4]. 5-FU acts as a thymidylate synthase inhibitor and blocks synthesis of the pyrimidine thymidylate, which is a nucleotide required for deoxyribonucleic acid (DNA) replication, resulting in cancerous cell death via thymineless death [4]. Currently, 5-FU is used in combination with other drugs and therapies for the treatment of many types of cancer, including stomach cancer, skin warts, breast cancer, cervical cancer, basal cell carcinoma, and colorectal esophageal cancer [5]. The combined use of 5-FU can maximize its effectiveness against some cancers; however, it may cause strong side effects that need to be addressed. And another point to note is that there is very little difference between the maximum tolerated dose and minimum effective dose of 5-FU because of side effects [6, 7]. Therefore, it is expected to clarify the causes and mechanisms of the side effects to secure diverse use of 5-FU as a combined therapy for cancer treatment.

As many immune checkpoint inhibitors are being developed, further development of immunotherapy is expected in the future, and combination with DNA analog drugs involving 5-FU has the potential to become a highly effective therapy. The immune system of the living body involves numerous proteins and cells such as neutrophils, macrophages, killer T cells, and various cytokines [8, 9]. Immunotherapy acts on any part of the complex immune system to increase its cytotoxic effect on cancer cells, while the terminal of the immune system oxidizes and destroys cancer cells by producing reactive oxygen species (ROS). Therefore, DNA analog drugs such as 5-FU are required to act under a lot of ROS produced in the immune system for the effect of replication inhibitor in the combined use. To maximize its effectiveness as the combined use, it is necessary to not degrade against ROS, but low degradation may increase side effects by increasing concentrations of 5-FU in blood plasma. Conversely, products derived from the oxidative degradation of 5-FU may cause side effects. In addition,

✉ Tatsushi Nakayama
tnakayama@gifu-pu.ac.jp

[1] Department of Pharmacy, Gifu Pharmaceutical University, 1-25-4 Daigaku-nishi, Gifu 501-1196, Japan

if most of the dosed 5-FU is decomposed, the concentration near the cancer cells drops to a level where the desired antimetabolite effect cannot be obtained. Considering the above, it is necessary to demonstrate the chemical reaction between 5-FU and ROS such as superoxide radical anion ($O_2^{\bullet-}$, a precursor of hydroperoxyl radical: $HO_2^{\bullet}$) and hydroxyl radical ($OH^{\bullet}$). That is, clarifying the chemical mechanism of the oxidative degradation of 5-FU by ROS is a prerequisite to elucidate the related medicinal side effects, since oxidized products may cause several pathologies.

Recently, Xiaofan Li et.al. investigated the oxidation mechanism of 5-FU by ozone (O_3) and $OH^{\bullet}$ using density functional theory (DFT) calculations to assess the potential ecotoxicology of 5-FU as a recalcitrant compound to the natural environment [10]. They clarified that 5-FU can be rapidly degraded by O_3 and $OH^{\bullet}$, which subsequently undergoes ring-opening, decomposition, defluorination, and hydroxylation steps, forming fifteen structures of transformation products, including five experimental products [11, 12]. Here, both O_3 and $OH^{\bullet}$ are particularly strong oxidants among ROS although are not main oxidants in living organisms. Thus, $O_2^{\bullet-}$, that is the majority in ROS produced by phagocytes (neutrophils, monocytes and macrophages) in the in vivo immune system, may be the oxidant for 5-FU degradation. Since $O_2^{\bullet-}$ is not a moderately good electrophile that can accept electrons from 5-FU, $HO_2^{\bullet}$ formed after protonation of $O_2^{\bullet-}$ as a Brønsted base is a strong oxidant with a short lifetime. Therefore, $HO_2^{\bullet}$ is inferred to be the actual oxidants in the living body, where proton transfer (PT) and electron transfer (ET) are closely related to the 5-FU oxidation mechanism. Several oxidation mechanisms of acidic 5-FU are possible, such as single–electron transfer (SET), superoxide-facilitated oxidation [13–15], sequential proton-loss electron transfer [16], and hydrogen–atom transfer (HAT) involving proton-coupled electron transfer (PCET) [17–20]. Currently, it is reasonable that HAT involving PCET is plausible for the oxidation of 5-FU rather than SET. In our previous studies, the PCET reaction between electrogenerated $O_2^{\bullet-}$ and acidic antioxidants was analyzed in an aprotic solvent [18, 20–27]. These studies suggested that even a recalcitrant compound such as 5-FU can be oxidized by $O_2^{\bullet-}$ or $HO_2^{\bullet}$ (protonated form of $O_2^{\bullet-}$) through a PCET mechanism initiated by the initial PT. Therefore, it is essential to reveal the detailed mechanism of the initial reaction between 5-FU and $O_2^{\bullet-}$ ($HO_2^{\bullet}$) because complicated metabolic reactions follow it forming the main transformation products in the living body, for evaluating the causes and mechanisms of the side effects.

In this study, the reaction mechanism between 5-FU and $O_2^{\bullet-}$ ($HO_2^{\bullet}$) in an aqueous environment was investigated using DFT calculations. Then, DFT results comparatively evaluated the degradability of 5-FU by $O_2^{\bullet-}$ ($HO_2^{\bullet}$) with those of two pyrimidine bases (Chart 1),

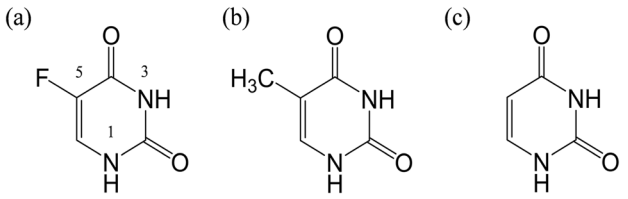

Chart 1 Structures of the compounds considered in the present study. **a** 5-Fluoro-1*H*,3*H*-pyrimidine-2,4-dione (5-fluorouracil), **b** 5-methylpyrimidine-2,4(1*H*,3*H*)-dione (thymine), and **c** pyrimidine-2,4(1*H*,3*H*)-dione (uracil)

5-methylpyrimidine-2,4(1*H*,3*H*)-dione (thymine), and pyrimidine-2,4(1*H*,3*H*)-dione (uracil, a nucleobase in ribonucleic acid: RNA). Accordingly, I present valuable information regarding the oxidative degradation of 5-FU by $O_2^{\bullet-}$ ($HO_2^{\bullet}$) in an aqueous environment simulating a living cell, which is assumed to be important for understanding the side effects and expanding the scope of 5-FU application.

Methods

Solution-phase DFT calculations were performed with two hybrid functionals, the Becke three-parameter Lee–Yang–Parr functional (B3LYP) and the Minnesota 06 functional (the meta exchange-correlated functional, M06-2X) [28], implemented in the Gaussian 16 Program package [29]. These functionals obtain good geometries for the reactants and products in PCET reactions between acidic substrates and free radicals [30]. I obtained the energies of the highest occupied molecular orbital (HOMO) and the lowest unoccupied molecular orbital (LUMO) from geometry optimization using frontier orbital theory. In the calculations, I applied the standard split-valence triple ζ basis sets augmented by the polarization 3df,2p and diffusion orbitals 6–311 + + G(3df,2p). The polarized continuum model (PCM) was employed for the solvent contribution of water to the standard Gibbs free energies under the default settings of Gaussian 16 that is widely employed. The internal energies were converted to standard Gibbs energies at 298.15 K using the zero-point energies, thermal correction, and entropy. The electrons and spins were obtained using the natural bond orbital (NBO) technique in population analysis [31].

Result and discussion

Optimization of stable structure of 5-FU and its deprotonate anion

To elucidate the reaction mechanism between 5-FU and $O_2^{\bullet-}$ in aqueous environments such as living organisms, DFT

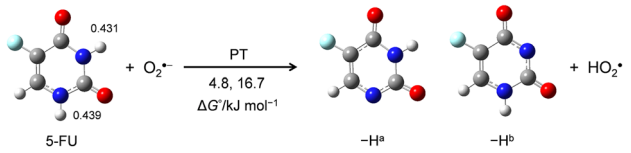

Fig. 1 Optimized structures of 5-fluorouracil (5-FU) and deprotonated anions ($-H^a$ and $-H^b$) along a proton transfer (PT) from its amine group at the first and third positions (1NH and 3NH) to $O_2^{\bullet-}$ in water, calculated using DFT-B3LYP/PCM/6–311 + + G(3df,2p) method. The $\Delta G°$s (kJ mol^{-1}, 298.15 K) of PT and charges distributed on the protons of 5-FU obtained in the NBO analysis are also indicated

calculations were performed using the B3LYP and M06-2X hybrid functionals employing the PCM method. Here, I focus on the B3LYP results because the results obtained using both functionals are similar. First, the stable structures of the possible reactant species, 5-FU, its deprotonated anion of two conformers ($-H^a$ and $-H^b$), $O_2^{\bullet-}$, and $HO_2^{\bullet}$, which coexist in aqueous cells, were obtained from energy scanning (Supporting Information, Tables S1–S4). Figure 1 shows the optimized structures with their calculated standard Gibbs free energy changes ($\Delta G°$/kJ mol^{-1}, 298.15 K) along the PT from 5-FU to $O_2^{\bullet-}$ (M06-2X results are shown in Supporting Information, Fig. S1). Charges distributed on the amine (NH) protons were obtained by NBO analysis.

In the living body, $O_2^{\bullet-}$ produced in the immune system acts as a Brønsted base though that accepts a proton from the aqueous environment, forming $HO_2^{\bullet}$. Conversely, $HO_2^{\bullet}$ is a strong oxidant with a short lifetime that cannot accept any more protons without accepting an electron. Therefore, $HO_2^{\bullet}$ immediately reacts with 5-FU only when generated in the vicinity of 5-FU molecule. Comparing the charges on the two NH protons of 5-FU at the first and third positions (1NH: 0.439 and 3NH: 0.431), it was observed that the proton reactivities in the acid–base reaction are slightly higher at 1NH than at 3NH. Similarly, the $\Delta G°$ values (kJ mol^{-1}) of the PT from 5-FU to $O_2^{\bullet-}$ indicate that deprotonation at 1NH forming $-H^a$ (4.8) is more feasible than that at 3NH forming $-H^b$ (16.7). According to these calculations, PT occurs at the 1NH of 5-FU toward $O_2^{\bullet-}$ depending on the acidity of the biological environment.

Change in HOMO–LUMO energies during PCET between 5-FU and $O_2^{\bullet-}$

The mechanistic analysis of reactivity between $O_2^{\bullet-}$ ($HO_2^{\bullet}$) and 5-FU in water was supplemented by frontier molecular orbital analysis based on DFT. Figure 2 shows the HOMO–LUMO (Hartree/a.u.) changes during PCET between 5-FU and $O_2^{\bullet-}$ (M06-2X results are shown in Supporting Information, Fig. S2). After the initial PT, the reactant species, 5-FU, $-H^a$, $O_2^{\bullet-}$, and $HO_2^{\bullet}$ coexist in the experimental solution. The HOMO energies of 5-FU (−0.25953) and its anion ($-H^a$: −0.20788) were much higher than the singly occupied molecular orbital (SOMO) energy of $HO_2^{\bullet}$ (−0.31427), indicating that the electron acceptor was $HO_2^{\bullet}$ rather than $O_2^{\bullet-}$ (−0.16005). Meanwhile, $HO_2^{\bullet}$ can be formed after PT to $O_2^{\bullet-}$ from aqueous solvent or 5-FU. Therefore, the electron donor was 5-FU or $-H^a$ (the bold red lines in Fig. 2 indicate the downhill energy relationship during the ET). Then, after the subsequent ET, the HOMO–LUMO relationship between the products (i.e., $-e/-H^a - e$ and HO_2^-) is reversed, as shown

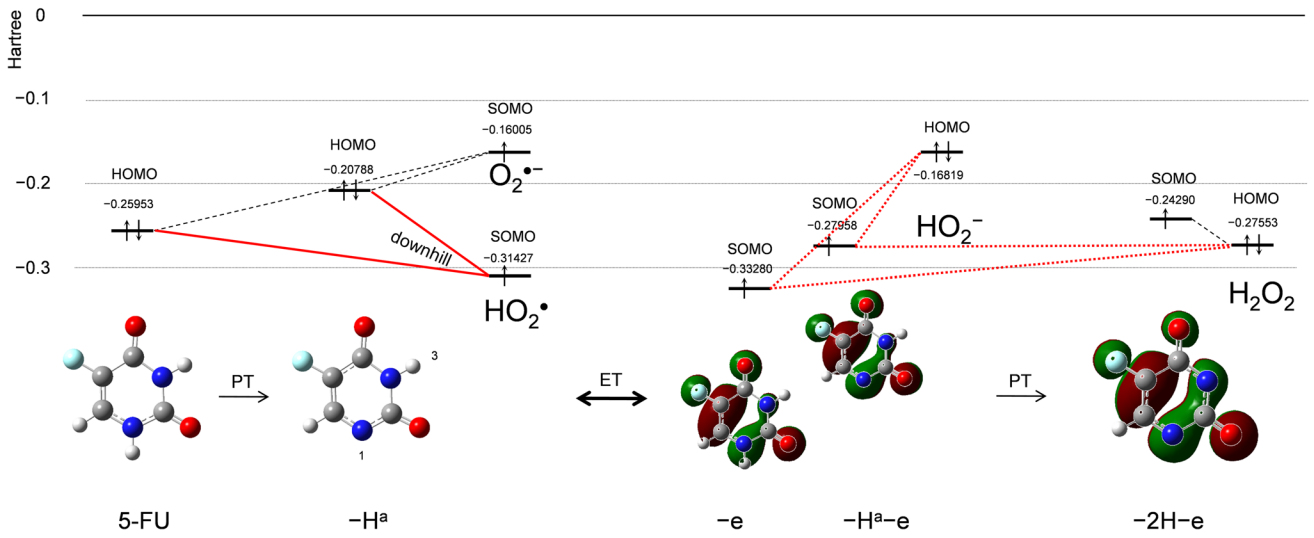

Fig. 2 Change in HOMO − LUMO energies (Hartree/a.u.) during proton-coupled electron transfer between 5-fluorouracil (5-FU) and $O_2^{\bullet-}$ in water, calculated using DFT-B3LYP/PCM/6–311 + + G(3df,2p) method

by the red dotted lines; thus, the reverse ET may proceed. However, H_2O_2 has a lower HOMO (−0.27553) than that of hydroperoxyl anion, HO_2^- (−0.16819), and a SOMO of radical anion,−2H−e (−0.24290), indicating that the second PT from neutral radical−H^a−e forming−2H−e prevents the reverse ET. Notably, the radical intermediates (radical cation: − e and − H^a − e) have very low SOMO (−0.33280 and −0.27958) comparable to that of $HO_2^{\bullet}$, which causes the reverse ET from HO_2^- or hydrogen peroxide (H_2O_2). This indicates that 5-FU is difficult to be oxidized and also suggests that intermediate radicals and anions may undergo subsequent reactions between another molecule of $O_2^{\bullet-}$ or $HO_2^{\bullet}$ (e.g., radical adduct formation) through pathways other than PCET. As a result of the mechanistic analysis using the HOMO–LUMO relationship, 5-FU is difficult to be oxidized by $O_2^{\bullet-}$ but $HO_2^{\bullet}$ through a PCET.

Δ*G*°s in PCET between 5-FU and $O_2^{\bullet-}$

For a thermodynamic analysis of the oxidation mechanism of 5-FU by $O_2^{\bullet-}$ in water, Δ*G*°s (kJ mol^{-1}, 298.15 K) along the PCET were obtained using solution-phase vibrational frequency calculations employing the PCM method (Supporting Information, Tables S1–S4). Figure 3 shows the equilibrium schemes and Δ*G*°s of the six diabatic electronic states in the PCET involving two PTs and one ET between 5-FU and $O_2^{\bullet-}$ calculated at the B3LYP/PCM/6–311 + + G(3df,2p) level (M06-2X results are shown in Table 1). Along the sequential pathway shown in Fig. 3, the main drivers are the Δ*G*°s of the individual reactions, the redox potentials (ET1–ET3), and the acid–base interactions (PT1–PT4) of the components. Since ET1 (472.8) is strongly endergonic, PT1 (4.8) dominantly forms –H^a and $HO_2^{\bullet}$. In the subsequent pathway (bottom of the panels in Fig. 3), both PT3 (352.5) and ET2 (116.5) are endergonic, so the sequential pathway is unlikely to proceed. However, PT3 and ET2 are promoted by the following exergonic processes, ET3 (− 306.9) and PT4 (− 70.9). As shown in the HOMO–LUMO relationship (Fig. 2), the second PT forming H_2O_2 is necessary for successful ET along the PCET. Therefore, it is rational that the proton and electron are transferred in one kinetic process corresponding to the diagonal of the rectangle in Fig. 3, labeled concerted PCET (45.6). Thus, the only feasible pathway is PT1 followed by concerted PCET rather than a sequential pathway of PT1–ET2–PT4 (PT1–PT3–ET3), resulting in the oxidative degradation of 5-FU by $O_2^{\bullet-}$. The Δ*G*° of the concerted PCET (45.6) is not high, although a prereactive step to form a hydrogen-bonded complex between –H^a (at 3NH) and $HO_2^{\bullet}$ is required. As a result of the thermodynamic analysis using the Δ*G*°s, 5-FU is possible to be oxidized by $O_2^{\bullet-}$, where $HO_2^{\bullet}$ preformed via the PT (4.8) acts as an actual oxidant through a concerted PCET mechanism which is a weakly endergonic pathway.

For a comparative study, the Δ*G*° values of the PCET pathways of thymine, uracil, and 5-FU with analog structures were calculated (Table 1). Thermodynamically, the

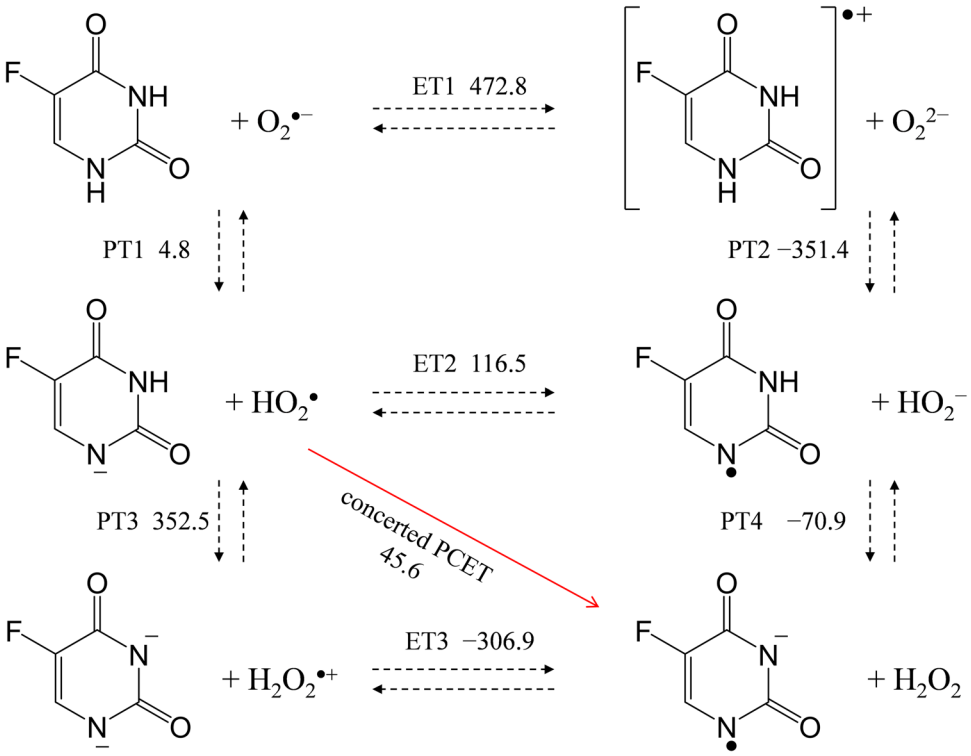

Fig. 3 Six diabatic electronic states of two proton transfers (PT1–PT4) and one electron transfer (ET1–ET3) between 5-fluorouracil and $O_2^{\bullet-}$ in water. The Δ*G*°s (kJ mol^{-1}, 298.15 K) were calculated using DFT-(U)B3LYP/PCM/6–311 + + G(3df,2p) method

Table 1 $\Delta G°$ values (kJ mol^{-1}, 298.15 K) of proton-coupled electron transfer between 5-fluorouracil (5-FU), thymine, uracil, and $O_2^{\bullet-}$ in water, calculated using DFT at the B3LYP and M06-2X functionals with the PCM/6–311 + + G(3df,2p) basis set

	Compounds	PT1[a]	PT2	PT3	PT4	ET1	ET2	ET3	Concerted[b]	Total[c]
B3LYP	5-FU[d]	4.8	−351.4	352.5	−70.9	472.8	116.5	−306.9	45.6	50.5
	Thymine	23.0	−326.7	371.2	−49.4	446.7	97.0	−323.6	47.6	70.6
	Uracil	17.4	−341.8	367.7	−56.1	482.9	123.6	−300.2	67.5	84.9
M06-2X	5-FU	−3.5	−374.7	349.6	−83.1	504.1	132.9	−299.8	49.8	46.3
	Thymine	14.0	−351.6	367.6	−62.3	482.1	116.5	−313.3	54.1	68.1
	Uracil	7.9	−363.7	364.7	−67.8	514.6	142.9	−289.6	75.1	83.0

[a]Proton transfer (PT1–PT4) and electron transfer (ET1–ET3)

[b]The values for concerted correspond to sums of those for ET2 and PT4 (PT3 and ET3)

[c]The values for total correspond to sums those for one ET and two PTs

[d]PT1 and PT2 occur from amine group at the first position and PT3 and PT4 at the third position of each compound

energetic driving force of the PCET is the sum of the $\Delta G°$s of the two PTs and one ET, although the sum cannot embody the energetic driving force if the PCET occurs along a pathway involving an infeasible single PT/ET. Along the plausible sequential pathway, PT1–ET2–PT4, the $\Delta G°$s of ET2 for each compound were strongly endergonic when using each of the B3LYP or M06-2X functionals. Thus, the $\Delta G°$ results imply that the initial PT (PT1) followed by a concerted PCET which correspond to sums of those for ET2 and PT4 (PT3 and ET3) is the most feasible pathway for the oxidation of each compound by $O_2^{\bullet-}$. Then, the $\Delta G°$s of the concerted PCET (concerted in Table 1) and the net PCET involving two PTs and one ET (total in Table 1) indicate that 5-FU (45.6, 50.5/49.8, 46.3) is more easily oxidized than thymine (47.6, 70.6/54.1, 68.1) and uracil (67.5, 84.8/75.1, 83.0) by $O_2^{\bullet-}$. Thus, this $\Delta G°$ results explain that 5-FU is comparatively more degradable by $O_2^{\bullet-}$ than uracil and thymine. In addition, 5-FU plays a preventive role in cellular oxidative damage at the pyrimidine base (uracil in RNA, thymine in DNA).

$\Delta G°$s in PCET between 5-FU and $HO_2^{\bullet}$

Next, a thermodynamic analysis of the oxidation mechanism of 5-FU by $HO_2^{\bullet}$ preformed via the protonation of $O_2^{\bullet-}$ in aqueous environment was conducted. Figure 4 shows the equilibrium schemes and $\Delta G°$s of the PCET involving one PT and one ET between 5-FU and $HO_2^{\bullet}$ calculated at the B3LYP/PCM/6–311 + + G(3df,2p) level (M06-2X results are shown in Table 2). PT occurs from 1NH (a) or 3NH (b) in 5-FU. In both cases, the concerted PCET (50.2, 105.2, red lines) is a feasible pathway because the initial processes of sequential pathways (ET–PT or PT–ET), ET1 (255.6) and PT1 (266.0, 277.9), are strongly endergonic. A comparison of these two $\Delta G°$s of the concerted PCET clearly suggests that the reaction proceeds at 1NH. Thus, it is rational that the proton and electron are transferred in one kinetic process at 1NH corresponding to the diagonal of the rectangle in Fig. 4a; labeled concerted.

In Table 2, the $\Delta G°$ values of the PCET between 5-FU, thymine, uracil, and $HO_2^{\bullet}$ calculated using the B3LYP or M06-2X functionals are compared. Similar to 5-FU, the $\Delta G°$ results indicate that the sequential pathways (ET1–PT2 or PT1–ET2) for thymine and uracil are unfeasible because the initial processes are strongly endergonic. Therefore, only the same concerted PCET pathway at 1NH can occur between $HO_2^{\bullet}$ and these pyrimidine bases. The $\Delta G°$ values of the concerted PCET indicate that 5-FU (50.2, 54.0) and thymine (48.9, 55.1) may be oxidized because of their weakly endergonic pathway showing similar reactivities toward $HO_2^{\bullet}$. During the reaction in water solution, a few elementary steps are assumed to proceed, generation of $HO_2^{\bullet}$ via protonation of $O_2^{\bullet-}$, formation of a prereactive complex (PRC) via a hydrogen bond (HB) from the free reactants (5-FU, thymine, uracil, and $HO_2^{\bullet}$), and the concerted PCET yielding product complex resulting in degradation of the pyrimidine analog. Considering that $HO_2^{\bullet}$ is a strong oxidant with a short lifetime, this series of steps must proceed with superior kinetics to oxidize 5-FU. This is because in cells in which a large amount of pyrimidine bases coexists, $HO_2^{\bullet}$ reacts with the pyrimidine bases or disappears through a dismutation reaction. Therefore, 5-FU cannot form the PRC in an experimental solution, resulting in not being oxidized by $HO_2^{\bullet}$, although the $\Delta G°$ results indicate that 5-FU and thymine can be oxidized through a concerted PCET.

Collectively, these $\Delta G°$ analyses indicate that the oxidation of 5-FU by $O_2^{\bullet-}$ or $HO_2^{\bullet}$ in water can proceed through the concerted PCET. Furthermore, two PCET pathways are feasible for the oxidation of 5-FU, the initial PT followed by a concerted PCET between 5-FU and $O_2^{\bullet-}$, and a concerted PCET between 5-FU and $HO_2^{\bullet}$ preformed via the protonation of $O_2^{\bullet-}$ by solvent-derived proton. In both pathways, a significant step is the formation of PRC via a HB between $HO_2^{\bullet}$ and 5-FU because the actual oxidant is $HO_2^{\bullet}$ with a short lifetime.

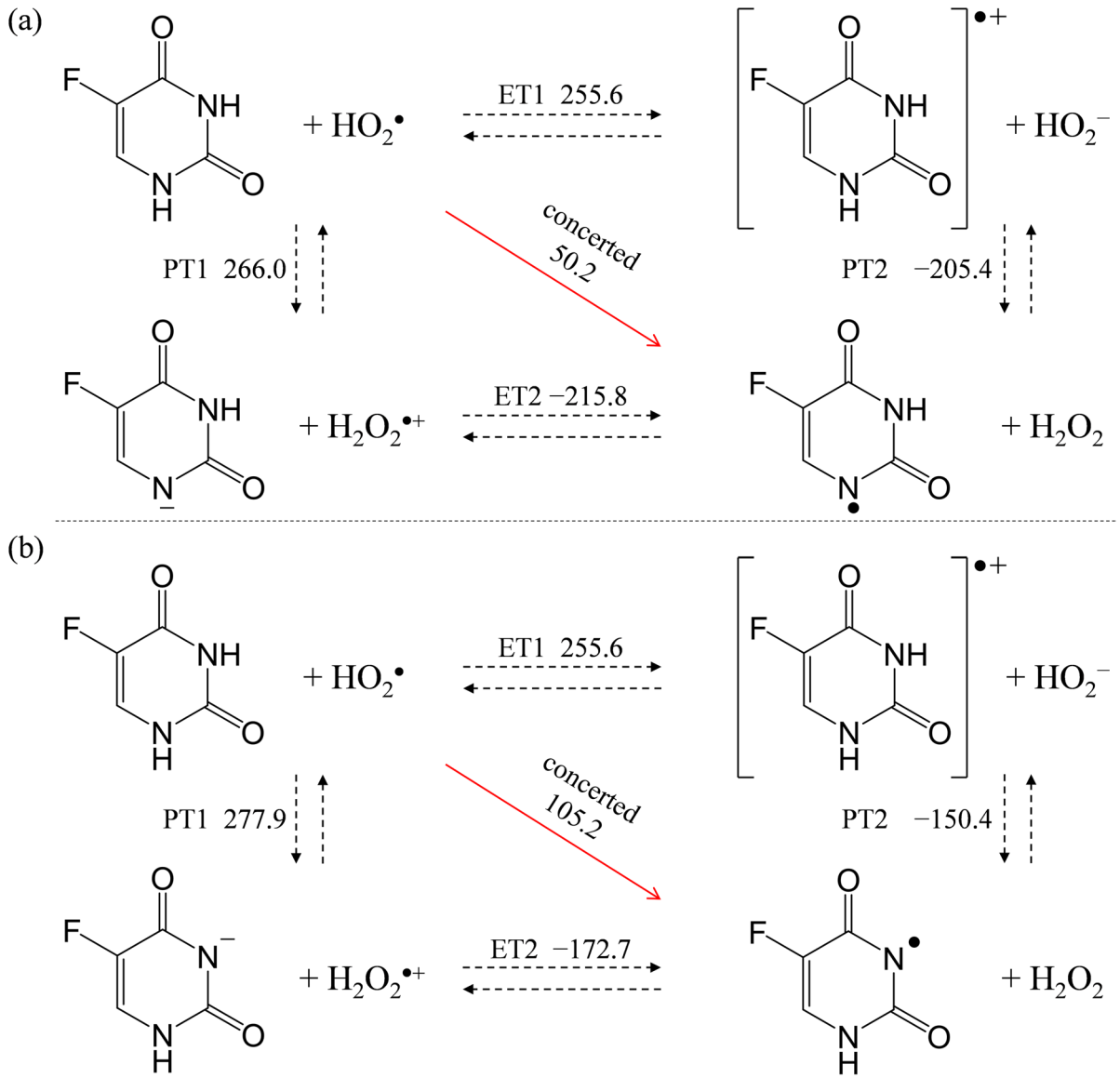

Fig. 4 Four diabatic electronic states of one proton transfer (PT1, PT2) and one electron transfer (ET1, ET2) between 5-fluorouracil and $HO_2^{\bullet}$ in water. The $\Delta G°$s (kJ mol^{-1}, 298.15 K) were calculated using DFT-(U)B3LYP/PCM/6–311 + + G(3df,2p) method

Analyses of reaction coordinates and potential-energy surfaces of the PCET between 5-FU and $HO_2^{\bullet}$

To infer the mechanistic insights of the oxidative degradation of 5-FU, I investigated the potential-energy surfaces of the PCET between 5-FU/−H and $HO_2^{\bullet}$ using the (U)B3LYP and M06-2X/PCM/6–311 + + G(3df,2p) levels of theory combined with NBO calculations. Here, I focus on the B3LYP results because the results obtained using both functionals are similar (M06-2X results are shown in Supporting Information, Fig. S3). During the reaction, the prereactive elementary steps are assumed to proceed, i.e., formation of $HO_2^{\bullet}$ and formation of PRC via HBs between 5-FU/−H and $HO_2^{\bullet}$. Then, PCET occurs, forming a product complex (PC) via TS. First, I scanned some plausible PRCs, the stable intermediate complex, TS, and PC, along with the concerted PCET reaction (Supporting Information, Table S5). As a result, only a 1:1 PRC formed between 5-FU and $HO_2^{\bullet}$ (5-FU—$HO_2^{\bullet}$) bonded at the 1NH (and auxiliary at oxygen atom at the second position) can form a PC (−H−e—H_2O_2) through the concerted PCET involving one ET and one PT along an intrinsic reaction coordinate (IRC) via a TS (Fig. 5). Figure 5a shows the energy profile ($\Delta G°$, kJ mol^{-1}) along the IRC, which forms the PC via the TS with an activation energy (E_a = 91.8 kJ mol^{-1}), where E_a is not so high energetic barrier. Then, the PC (62.1) dissociates yielding −H−e and H_2O_2 as the free products (FP, 41.0). Here, −H−e is a neutral radical that is expected to undergo

Table 2 ΔG^{o} values (kJ mol^{-1}, 298.15 K) of proton-coupled electron transfer between 5-fluorouracil (5-FU), thymine, uracil, and $HO_2^{\bullet}$ in water, calculated using DFT at the B3LYP and M06-2X functionals with the PCM/6–311 + + G(3df,2p) basis set

	Compounds	[a]Position	[b]PT1	PT2	ET1	ET2	[c]Concerted
B3LYP	5-FU	1NH	266.0	−205.4	255.6	−215.8	50.2
		3NH	277.9	−150.4	255.6	−172.7	105.2
	Thymine	1NH	284.2	−180.6	229.5	−235.3	48.9
		3NH	298.5	−125.7	229.5	−194.7	103.8
	Uracil	1NH	278.6	−195.7	265.6	−208.7	69.9
		3NH	294.6	−136.1	265.6	−165.1	129.5
M06-2X	5-FU	1NH	264.0	−220.9	275.0	−209.9	54.0
		3NH	274.3	−162.6	275.0	−161.8	112.4
	Thymine	1NH	281.5	−197.9	253.0	−226.4	55.1
		3NH	294.3	−139.5	253.0	−180.8	113.5
	Uracil	1NH	275.5	−210.0	285.5	−199.9	75.5
		3NH	290.9	−147.2	285.5	−152.6	138.3

[a]Reaction site of the compounds for PT1, PT2, and concerted PCET and amine groups at the first position, 1NH, and the third position, 3NH

[b]Proton transfer (PT1–PT2) and electron transfer (ET1–ET2)

[c]The values for concerted correspond to sums of those for ET1 and PT2 (PT1 and ET2)

various subsequent reactions and be easily decomposed in an aqueous environment.

Figure 5b shows the dependence of N – H bond distance (1 N – H, black line, nm) on the number of electrons in the π-orbital of the planar 5-FU molecule along the IRC (blue circles). The spin density distributions were localized on the radicals before and after the TS along the concerted PCET, demonstrating that the radical localized on $HO_2^{\bullet}$ in the initial PRC was transferred to – H – e (5-FU side) in the resulting PC. The spin changes on the electron-donor side (5-FU) and electron-acceptor side ($HO_2^{\bullet}$) were well correlated with the changes in the π-electrons of 5-FU. The spins also demonstrate that the TS is electronically characterized by the delocalization of the π-electrons over the HB complex of the components. As a result, IRC revealed that an intracomplex PCET between 5-FU (at 1NH) and $HO_2^{\bullet}$ occurs in a concerted one-kinetic process without generating intermediates.

Collectively, these findings indicate that the oxidation of 5-FU by $O_2^{\bullet-}$ in water is governed by the concerted PCET after the formation of PRC between 5-FU and preformed $HO_2^{\bullet}$ via HBs at 1NH, which corresponds to moving along the red diagonal lines in Fig. 4a.

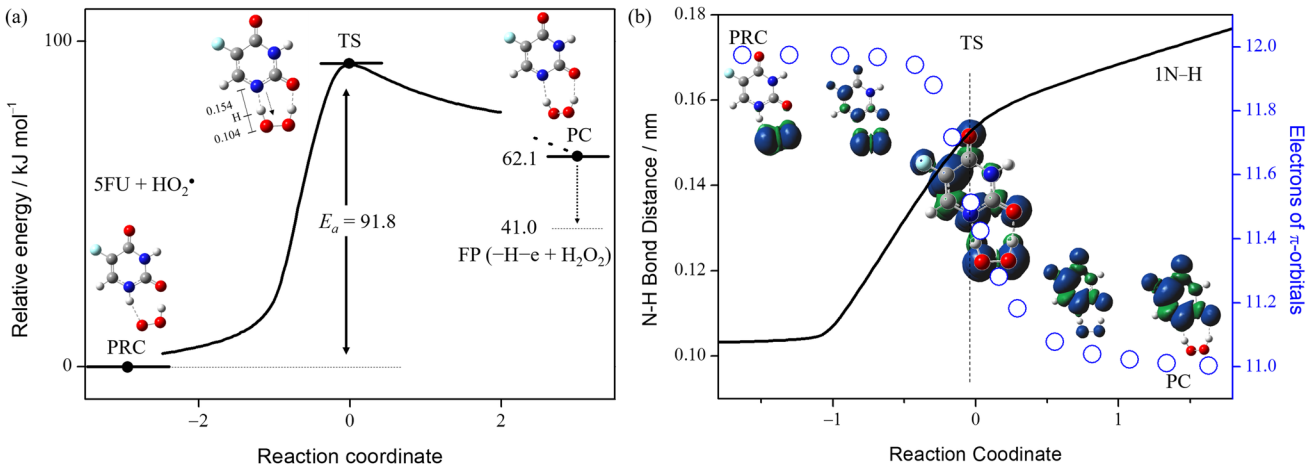

Fig. 5 **a** Energy profile (kJ mol^{-1}, 298.15 K) along the reaction coordinate of proton-coupled electron transfer between 5-fluorouracil (5-FU) and $HO_2^{\bullet}$ in water with the structures of prereactive complex (PRC, 5-FU—$HO_2^{\bullet}$), transition state (TS), and product complex (PC, – H – e—H_2O_2), forming free products (FP). **b** Changes in N – H bond distance (1 N – H: black line, nm), and the number of electrons (open circles) in the π-orbitals of 5-FU, corresponding to the labels of the left and right vertical axes. Calculations were performed using the DFT-(U)B3LYP/PCM/6–311 + + G(3df,2p) method. The spin distributions of the complexes obtained from the NBO analyses are demonstrated

Conclusions

In conclusion, I clarified the initial reaction between 5-FU and $O_2^{\bullet-}$ ($HO_2^{\bullet}$) in water solutions using DFT calculations, which is expected to lead to the degradation of 5-FU and complicated metabolic reactions. The main findings are summarized below:

1. Oxidation of 5-FU by $O_2^{\bullet-}$ or $HO_2^{\bullet}$ in water is feasible through the PCET mechanism.
2. A concerted PCET between 5-FU and $HO_2^{\bullet}$ preformed via the protonation of $O_2^{\bullet-}$ involving one PT and one ET in one kinetic process is a plausible pathway.
3. The actual oxidant of 5-FU along the PCET mechanism is $HO_2^{\bullet}$.

These findings using DFT calculations revealed the PCET mechanism of 5-FU oxidation by $O_2^{\bullet-}$ and $HO_2^{\bullet}$, which cannot be observed in water or aqueous in vivo experiments. I hope that these findings will provide mechanistic insight into the biodegradability of 5-FU through oxidation by $O_2^{\bullet-}$, securing the pharmacological use of 5-FU.

Abbreviations DFT: Density functional theory; PCET: Proton-coupled electron transfer; ROS: Reactive oxygen species; PT: Proton transfer; ET: Electron transfer; SET: Single-electron transfer; HAT: Hydrogen-atom transfer; B3LYP: Becke three-parameter Lee–Yang–Parr; M06-2X: Minnesota 06; HOMO: Highest occupied molecular orbital; LUMO: Lowest unoccupied molecular orbital; PCM: Polarized continuum model; NBO: Natural bond orbital; NH: Amine group; SOMO: Singly occupied molecular orbital; PRC: Prereactive complex; HB: Hydrogen bond

Supplementary Information The online version contains supplementary material available at https://doi.org/10.1007/s11224-023-02248-3.

Acknowledgements The authors would like to thank Yuki Mori for his experimental assistance.

Funding This research was funded by Iwatani Naoji Foundation, Research Foundation for the Electrotechnology of Chubu, and a Grant-in-Aid for Scientific Research, grant number 19K16338, from the Japan Society for the Promotion of Science (JSPS).

Availability of data and materials All data generated or analyzed during this study are included in this published article and its supplementary materials.

Declarations

Ethical approval Not applicable.

Competing interests The author declares no competing interests.

References

1. Azwar S, Seow HF, Abdullah M et al (2021) Recent updates on mechanisms of resistance to 5-fluorouracil and reversal strategies in colon cancer treatment. Biology (Basel) 10:854. https://doi.org/10.3390/biology10090854
2. Entezar-Almahdi E, Mohammadi-Samani S, Tayebi L, Farjadian F (2020) Recent advances in designing 5-fluorouracil delivery systems: a stepping stone in the safe treatment of colorectal cancer. Int J Nanomedicine 15:5445–5458. https://doi.org/10.2147/IJN.S257700
3. Sethy C, Kundu CN (2021) 5-Fluorouracil (5-FU) resistance and the new strategy to enhance the sensitivity against cancer: implication of DNA repair inhibition. Biomed Pharm 137. https://doi.org/10.1016/j.biopha.2021.111285
4. Longley DB, Harkin DP, Johnston PG (2003) 5-Fluorouracil: mechanisms of action and clinical strategies. Nat Rev Cancer 3:330–338. https://doi.org/10.1038/nrc1074
5. Yen Moore A (2009) Clinical applications for topical 5-fluorouracil in the treatment of dermatological disorders. J Dermatol Treat 20:328–335. https://doi.org/10.3109/09546630902789326
6. Gamelin E, Boisdron-Celle M (1999) Dose monitoring of 5-fluorouracil in patients with colorectal or head and neck cancer—status of the art. Crit Rev Oncol Hematol 30:71–79. https://doi.org/10.1016/S1040-8428(98)00036-5
7. Felici A, Verweij J, Sparreboom A (2002) Dosing strategies for anticancer drugs: the good, the bad and body-surface area. Eur J Cancer 38:1677–1684. https://doi.org/10.1016/S0959-8049(02)00151-X
8. Venter C, Eyerich S, Sarin T, Klatt KC (2020) Nutrition and the immune system: a complicated tango. Nutrients 12:818. https://doi.org/10.3390/nu12030818
9. Zoghi S, Masoumi F, Rezaei N (2023) The immune system. In: Clinical Immunology. Academic Press, pp 1–46
10. Li X, Lv G, Wang N et al (2022) Theoretical insights into the transformation mechanism and eco-toxicity effects of 5-Fluorouracil by O3 and ·OH in waters. Process Saf Environ Prot 160:541–550. https://doi.org/10.1016/J.PSEP.2022.02.045
11. Javitt L, Dror I, Berkowitz B (2019) Catalytic degradation of fluorouracil and its derivatives by copper-based nanoparticles. Environ Eng Sci 36:1466–1473. https://doi.org/10.1089/ees.2019.0210
12. Governo M, Santos MSF, Alves A, Madeira LM (2017) Degradation of the cytostatic 5-fluorouracil in water by Fenton and photo-assisted oxidation processes. Environ Sci Pollut Res 24:844–854. https://doi.org/10.1007/s11356-016-7827-2
13. Nanni EJ, Birge RR, Hubbard LM et al (1981) Oxidation and dismutation of superoxide ion solutions to molecular oxygen. singlet vs. triplet state. Inorg Chem 20:737–741. https://doi.org/10.1021/ic50217a019
14. Nanni EJ, Stallings MD, Sawyer DT (1980) Does superoxide ion oxidize catechol, α-tocopherol, and ascorbic acid by direct electron transfer? J Am Chem Soc 102:4481–4485. https://doi.org/10.1021/ja00533a029
15. Song C, Zhang J (2008) Electrocatalytic oxygen reduction reaction. PEM Fuel Cell Electrocatalysts and Catalyst Layers. Springer, London, pp 89–134
16. Biela M, Rimarčík J, Senajová E et al (2020) Antioxidant action of deprotonated flavonoids: thermodynamics of sequential proton-loss electron-transfer. Phytochemistry 180. https://doi.org/10.1016/j.phytochem.2020.112528
17. Singh PS, Evans DH (2006) Study of the electrochemical reduction of dioxygen in acetonitrile in the presence of weak acids. J Phys Chem B 110:637–644. https://doi.org/10.1021/jp055296f

18. Nakayama T, Uno B (2015) Importance of proton-coupled electron transfer from natural phenolic compounds in superoxide scavenging. Chem Pharm Bull (Tokyo) 63:967–973. https://doi.org/10.1248/cpb.c15-00447
19. Nakayama T, Uno B (2016) Structural properties of 4-substituted phenols capable of proton-coupled electron transfer to superoxide. Int J Adv Res Chem Sci 3:11–19. https://doi.org/10.20431/2349-0403.0301002
20. Nakayama T, Uno B (2022) Reactivities of hydroxycinnamic acid derivatives involving caffeic acid toward electrogenerated superoxide in *N*, N-dimethylformamide. Electrochem 3:347–360. https://doi.org/10.3390/electrochem3030024
21. Nakayama T, Uno B (2023) Reactivity of trans-resveratrol toward electrogenerated superoxide in N, N-dimethylformamide. J Agric Food Chem 71:4382–4393. https://doi.org/10.1021/acs.jafc.2c08105
22. Nakayama T, Uno B (2022) Reactivities of 1,2-, 1,3-, and 1,4-dihydroxynaphthalenes toward electrogenerated superoxide in *N*, N-dimethylformamide through proton-coupled electron transfer. Electrochim Acta 436:141467. https://doi.org/10.1016/J.ELECTACTA.2022.141467
23. Nakayama T, Honda R (2021) Electrochemical and mechanistic study of superoxide elimination by Mesalazine through proton-coupled electron transfer. Pharmaceuticals 14:120. https://doi.org/10.3390/ph14020120
24. Nakayama T, Honda R (2021) Electrochemical and mechanistic study of oxidative degradation of favipiravir by electrogenerated superoxide through proton-coupled electron transfer. ACS Omega 6:21730–21740. https://doi.org/10.1021/acsomega.1c03230
25. Nakayama T, Uno B (2016) Concerted two-proton-coupled electron transfer from catechols to superoxide via hydrogen bonds. Electrochim Acta 208:304–309. https://doi.org/10.1016/j.electacta.2016.05.034
26. Nakayama T, Honda R, Kuwata K et al (2022) Electrochemical and mechanistic study of reactivities of α-, β-, γ-, and δ-tocopherol toward electrogenerated superoxide in *N*, N-dimethylformamide through proton-coupled electron transfer. Antioxidants 11:115–128. https://doi.org/10.3390/antiox11010009
27. Nakayama T, Honda R, Kuwata K et al (2022) Electrochemical and mechanistic study of superoxide scavenging by pyrogallol in *N*, N-dimethylformamide through proton-coupled electron transfer. Electrochem 3:115–128. https://doi.org/10.3390/electrochem3010008
28. Zhao Y, Truhlar DG (2008) The M06 suite of density functionals for main group thermochemistry, thermochemical kinetics, noncovalent interactions, excited states, and transition elements: two new functionals and systematic testing of four M06-class functionals and 12 other function. Theor Chem Acc 120:215–241. https://doi.org/10.1007/s00214-007-0310-x
29. Frisch MJ, Trucks GW, Schlegel HB et al (2016) Gaussian 16, Rev. B.01. Gaussian, Inc.: Wallingford, CT, USA
30. Quintero-Saumeth J, Rincón DA, Doerr M, Daza MC (2017) Concerted double proton-transfer electron-transfer between catechol and superoxide radical anion. Phys Chem Chem Phys 19:26179–26190. https://doi.org/10.1039/c7cp03930a
31. Reed AE, Weinstock RB, Weinhold F (1985) Natural population analysis. J Chem Phys 83:735–746. https://doi.org/10.1063/1.449486